


Article

Dynamic Risk Assessment of High Slope in Open-Pit Coalmines Based on Interval Trapezoidal Fuzzy Soft Set Method: A Case Study

Zhiliu Wang ^{1,*} , Mengxin Hu ¹, Peng Zhang ², Xinming Li ¹ and Song Yin ¹

¹ School of Civil Engineering and Architecture, Zhongyuan University of Technology, Zhengzhou 450007, China

² CHN Baorixile Energy Co., Ltd., Hulunbuir 021599, China

* Correspondence: 6855@zut.edu.cn

Abstract: Effective high slope risk assessment plays an important role in the safety management and control of the open-pit coal mining process. Traditional slope stability risk assessment methods rarely consider the time factor or evaluate the dynamic change of high slope in an open-pit mine at a certain time in a sensitivity assessment. This paper develops an interval trapezoidal fuzzy soft set method to achieve the high slope dynamic risk evaluation. The proposed dynamic interval trapezoidal fuzzy soft set method for risk assessment of high slope in an open-pit coal mine is developed by integrating the time points and weights of slope risk factors. The extended interval trapezoidal fuzzy soft set was used to calculate the weights of risk factors at different times, and the Fuzzy Analytical Hierarchy Process (FAHP) method was applied to determine the weights of risk factors. The weight change of different risk factors with time can be easily achieved with the proposed method. As a case study, this approach is implemented into a risk assessment model for the north high slope in Shengli #1 open-pit mine located in Xilinhot, Inner Mongolia. The model complies with three time points and contains 4 primary risk factors (S) and 17 secondary risk factors. The results indicated that the hydrological climate conditions and slope geometry conditions were the high risk factors affecting this open-pit coal mine slope. The reasonability and effectiveness of the evaluation results were verified with in-situ observations and measurements. This dynamic risk assessment method is helpful for improving safety management and control for the high slopes of open-pit mines in the coal mining process.

Keywords: dynamic risk assessment; safety management and control; high slope; open-pit coalmine



Citation: Wang, Z.; Hu, M.; Zhang, P.; Li, X.; Yin, S. Dynamic Risk Assessment of High Slope in Open-Pit Coalmines Based on Interval Trapezoidal Fuzzy Soft Set Method: A Case Study. *Processes* **2022**, *10*, 2168. <https://doi.org/10.3390/pr10112168>

Academic Editors: Feng Du, Aitao Zhou and Bo Li

Received: 22 September 2022

Accepted: 20 October 2022

Published: 23 October 2022

Publisher's Note: MDPI stays neutral with regard to jurisdictional claims in published maps and institutional affiliations.



Copyright: © 2022 by the authors. Licensee MDPI, Basel, Switzerland. This article is an open access article distributed under the terms and conditions of the Creative Commons Attribution (CC BY) license (<https://creativecommons.org/licenses/by/4.0/>).

1. Introduction

In the current process of coal mining, coal mine disasters occur frequently, including landslides, gas explosion, the collapse of the roof, and rock burst, etc., whilst landslides are the dominant disaster type for the open-pit coalmine [1–3]. Slope stability directly affects coal mining safety. Especially for the high slope in the open-pit coalmine, where the height is generally over 200 m, a landslide disaster is more likely to occur because of complex geological conditions and multiple risk factors [4]. Accurate assessment and analysis of high slope stability in an open-pit mine is very important for landslide disaster prevention and control [5,6].

Slope stability analysis usually involves various uncertain factors, such as the statistical uncertainty of rock and soil parameters. However, conventional deterministic analyses, which use a factor of safety (FS) as the slope stability criterion, cannot quantitatively and comprehensively consider the influence of these uncertain factors [7–9]. Many scholars have tried to use different monitoring technologies to realize slope dynamic early warning, such as displacement information integration [10], synthetic aperture radar interference [11], ground-based synthetic aperture radar technology [12], and multi-technology

combination [13], etc. However, these monitoring techniques lack multivariate risk factors analysis. By contrast, risk assessment based on statistics and probability theory can reasonably and comprehensively quantify these uncertainties in slope stability analysis. The most frequently used analytical methods are probability theory [14–17], interval number theory [18], fuzzy theory [19–22], rough set theory, etc. [23,24], and direct MonteCarlo simulation (MCS) [25–27]. However, these methods cannot accurately solve the complex problem of slope risk assessment in which multiple factors and a large number of field data are involved. In recent years, analytic hierarchy process (AHP) [28–30] has been applied to systematically assess the slope stability. Santos et al. [31] proposed a hazard graph and generated the quantitative hazard assessment system to carry out risk analysis for open-pit mine slopes and saw the method as having a high discrimination capacity. Cheng et al. [32] used the random finite difference method (RFDM) to assess the risk of slope failure and concluded that the structure had a dual effect on the stability of the slope. Pinheiro et al. [33] developed slope quality Index and applied it to many real road slopes. Soft set theory also was used to study slope stability affected by multiple risk factors. Yang et al. [34] applied soft set theory to optimize the measures of highway slope treatment, and in their work the weights of affecting factors used in the slope safety evaluation were given by different experts. Fuzzy analytic hierarchy process (FAHP) determines the relative importance of each criterion through pairwise comparison given by domain experts or decision makers and is widely used to calculate standard weights [35–38]. In addition, Zhang and his co-researchers generalized parametric soft sets to dynamic interval trapezoidal fuzzy soft sets and made comprehensive evaluation decisions. The simultaneous feasibility of the decision-making method is proved by a case study [39]. The dynamic fuzzy soft set is also expanded into dynamic interval-valued fuzzy soft sets by He and his co-authors [40]. The operations and properties of dynamic interval-valued fuzzy soft set are studied, and the dynamic interval-valued fuzzy soft set decision is proposed. Zhu et al. enriched and improved the theory of interval trapezoidal fuzzy soft sets and promoted its practical application [41]. All of these achievements for statistics and probability theory have illustrated its capability and popularity in slope reliability analysis.

However, the studies rarely considered the factor of time in their sensitivity evaluation. Thus, the risk assessment of high slope cannot fully reflect the dynamic change of high slope in an open-pit coal mine during a certain period of time. For a slope in an open-pit coal mine, the change of slope stability at different time points is of great importance in risk management. In this work, an interval trapezoidal fuzzy soft set method is developed to achieve the high slope dynamic risk evaluation. The proposed dynamic interval trapezoidal fuzzy soft set method for risk assessment of high slope is developed by integrating time points and the weights of slope risk factors. More specifically, the time period is firstly clarified when the risk factors affecting the slope stability of open-pit mine are strongly superimposed. Then, the risk evaluation grade of the high slope is determined by the FAHP method, which determines slope risk factors by referring to the relevant specifications of the open-pit mine. The risk evaluation grade of the high slope is determined by the FAHP method. Again, the slope risk factors are quantified by expert scoring, and the weight of each risk factor is calculated by FAHP. The weight is independent of time. Then, the dynamic interval trapezoidal fuzzy soft set method is used to integrate the time and weights of different risk factors, and the entropy matrix is used to calculate the evaluation value of risk factors at different moments. The following, the multi-attribute decision integration and evaluation of all risk factor parameters in all time periods are carried out by the dynamic interval trapezoidal fuzzy soft set method. Finally, the high slope in the Shengli open-pit coal mine was taken as a case study, three time points were selected, and the parameter values of 17 secondary indicators were obtained. The risk factors of the high slope at different time points were evaluated and then verified with the field data monitored.

2. Expansion of Interval Trapezoidal Fuzzy Soft Sets

2.1. Interval Trapezoidal Fuzzy Soft Sets and Their Properties

In this section, we introduced some basic definitions and their properties in interval trapezoidal fuzzy soft set theory [42,43].

Definition 1. Let U be an initial universe set and E be a set of parameters. A denotes an interval trapezoidal fuzzy soft set over a common universe U . A is a subset of E , and $A \subset E$. A pair (F, A) is called an interval trapezoidal fuzzy soft set over a common universe U , where F is a mapping given by $F: A \rightarrow \Gamma(U)$.

That is to say, for $\forall e \in A$, we can obtain

$$F(e) = \left\{ \left\langle x, S_{F(e)}(x) \mid x \in U \right\rangle \right\} \quad (1)$$

where $S_{F(e)}(x)$ is the interval trapezoidal fuzzy number corresponding to x in $F(e)$.

Definition 2. Let (F, A) and (G, B) be interval trapezoidal fuzzy soft sets over a common universe U . (H, C) is the intersection of (F, A) and (G, B) , where $C = A \cap B$ and $(F, A) \cap (G, B) = (H, C)$. For $\forall \xi \in C$, we can obtain,

$$F(\xi) = F(\xi) \cap G(\xi) = \left\{ \left\langle x, S_{F(\xi)}(x) \cap S_{G(\xi)}(x) \mid x \in U \right\rangle \right\} \quad (2)$$

where $S_{F(\xi)}(x)$ and $S_{G(\xi)}(x)$ are the interval trapezoidal fuzzy Numbers corresponding to x in $F(\xi)$ and $G(\xi)$.

Definition 3. Let (F, A) and (G, B) be interval trapezoidal fuzzy soft sets over a common universe U . The union of (F, A) and (G, B) is defined as the soft set (M, D) , where $D = A \cup B$ and $(F, A) \cup (G, B) = (M, D)$. For $\forall \varepsilon \in D$, we can have

$$M(\varepsilon) = F(\varepsilon) \cup G(\varepsilon) = \left\{ \left\langle x, S_{M(\varepsilon)}(x) \mid x \in U \right\rangle \right\} \quad (3)$$

Among them

$$S_{M(\varepsilon)}(x) = \begin{cases} S_{F(\varepsilon)}(x), \varepsilon = A - B \\ S_{G(\varepsilon)}(x), \varepsilon = B - A \\ S_{F(\varepsilon)}(x) \cup S_{G(\varepsilon)}(x), \varepsilon = A \cap B \end{cases} \quad (4)$$

where $S_{F(\varepsilon)}(x)$ and $S_{G(\varepsilon)}(x)$ are the interval trapezoidal fuzzy numbers corresponding to x in $F(\varepsilon)$ and $G(\varepsilon)$, respectively.

If (G_1, A_1) and (G_2, A_2) are two interval trapezoidal fuzzy soft sets over a common universe U , then (G_1, A_1) and (G_2, A_2) is defined as

$$(G_1, A_1) \wedge (G_2, A_2) = (H, A_1 \times A_2) \quad (5)$$

We can obtain

$$H(\alpha, \beta) = G_1(\alpha) \cap G_2(\beta) = \left\{ \left\langle x, S_{G_1(\alpha)}(x) \cap S_{G_2(\beta)}(x) \mid x \in U \right\rangle \right\} \quad (6)$$

for $\forall (\alpha, \beta) \in A_1 \times A_2$, where $S_{G_1(\alpha)}(x)$ and $S_{G_2(\beta)}(x)$ are the interval trapezoidal fuzzy numbers of x in the $G_1(\alpha)$ and $G_2(\beta)$, respectively.

If (G_1, A_1) and (G_2, A_2) are two interval trapezoidal fuzzy soft sets over a common universe U , (G_1, A_1) or (G_2, A_2) is defined as

$$(G_1, A_1) \vee (G_2, A_2) = (M, A_1 \times A_2) \quad (7)$$

We can obtain

$$M(\alpha, \beta) = G_1(\alpha) \cup G_2(\beta) = \left\{ \left\langle x, S_{G_1(\alpha)}(x) \cup S_{G_2(\alpha)}(x) \right\rangle \mid x \in U \right\} \text{ for } \forall (\alpha, \beta) \in A_1 \times A_2 \quad (8)$$

where $S_{G_1(\alpha)}(x)$ and $S_{G_2(\alpha)}(x)$ are the interval trapezoidal fuzzy numbers of x in the $G_1(\alpha)$ and $G_2(\beta)$, respectively.

2.2. Correlation Theorem of Interval Trapezoidal Fuzzy Soft Sets

Theorem 1. If (G_1, A_1) , (G_2, A_2) and (G_3, A_3) are three interval trapezoidal fuzzy soft sets over a common universe U , we can obtain

$$((G_1, A_1) \vee (G_2, A_2)) \vee (G_3, A_3) = (G_1, A_1) \vee ((G_2, A_2) \vee (G_3, A_3)) \quad (9)$$

$$((G_1, A_1) \wedge (G_2, A_2)) \wedge (G_3, A_3) = (G_1, A_1) \wedge ((G_2, A_2) \wedge (G_3, A_3)) \quad (10)$$

Theorem 2. If (G_1, A_1) and (G_2, A_2) are two interval trapezoidal fuzzy soft sets over a common universe U , we can obtain

$$((G_1, A_1) \vee (G_2, A_2))^c = (G_1, A_1)^c \wedge (G_2, A_2)^c \quad (11)$$

$$((G_1, A_1) \wedge (G_2, A_2))^c = (G_1, A_1)^c \vee (G_2, A_2)^c \quad (12)$$

Theorem 3. If (G_1, A_1) , (G_2, A_2) and (G_3, A_3) are three interval trapezoidal fuzzy soft sets over a common universe U , we can obtain

$$((G_1, A_1) \vee (G_2, A_2)) \wedge (G_3, A_3) = ((G_1, A_1) \wedge (G_3, A_3)) \vee ((G_2, A_2) \wedge (G_3, A_3)) \quad (13)$$

$$((G_1, A_1) \wedge (G_2, A_2)) \wedge (G_3, A_3) = ((G_1, A_1) \vee (G_3, A_3)) \wedge ((G_2, A_2) \vee (G_3, A_3)) \quad (14)$$

Based on the above expansion of interval trapezoidal fuzzy soft sets, the dynamic risk evaluation model of high slope in an open-pit mine are established in the next section.

3. Establishing the Dynamic Risk Evaluation Model of High Slope in Open-Pit Mine

In this section, the following steps are used to integrate the time points and weights of slope risk factors (see Figure 1).

Step 1: Make clear the time period when the risk factors affecting the slope stability of open-pit mine are strong superimposed.

Step 2: Determine slope risk factors by referring to the relevant specifications of open-pit mine. They are technical specification for annual evaluation of the stability of open-pit coal mine slopes (GB/T 37573-2019) and code for the design of open-pit mines in the coal industry (GB 50197-2015). Then, the risk evaluation grade of high slope is determined by the FAHP method.

Step 3: The slope risk factors are quantified by expert scoring, and the weight of each risk factor is determined by FAHP method.

Step 4: The time and weight of risk factors are integrated by dynamic interval trapezoidal fuzzy soft sets, and the evaluation value of risk factors at different moments is calculated by entropy matrix. Finally, the multi-attribute decision integration and evaluation of all risk factor parameters in all time periods are carried out by dynamic interval trapezoidal fuzzy soft sets.

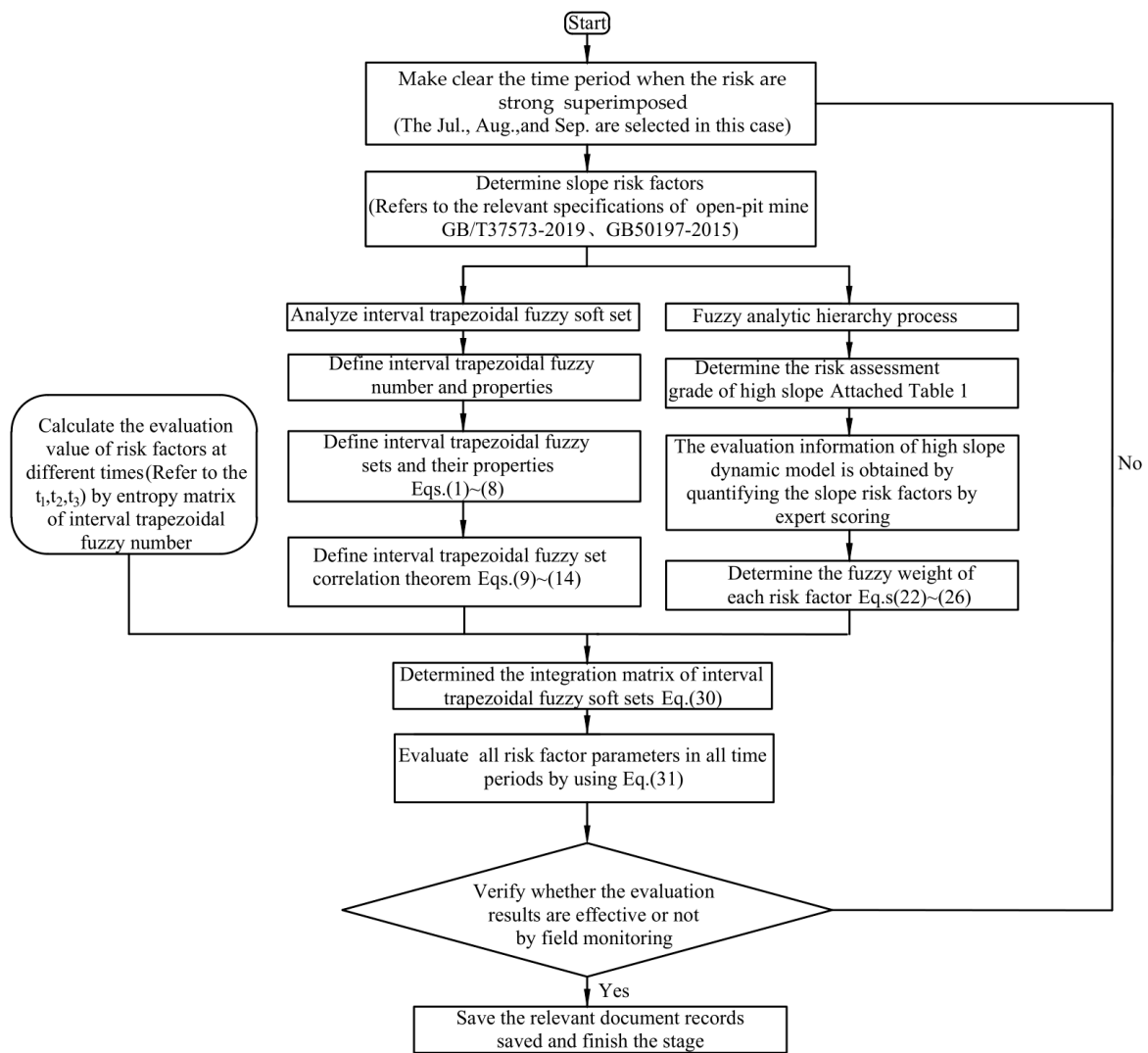


Figure 1. Intuitionistic trapezoidal fuzzy soft set method for risk assessment of high slopes.

For the dynamic evaluation of high slope risk in open-pit mine, the time point sets of monitoring data are given, which is denoted as

$$T = \{t_1, t_2, \dots, t_k\} \tag{15}$$

where t is the time point of different risk factors; k is the number of time points.

To determine four primary indexes, we mainly refer to the relevant specifications of open-pit mine, which are technical specification for annual evaluation of the stability of open-pit coal mine slopes (GB/T 37573-2019) and specifications for design of open pit mine of coal industry (GB 50197-2015). To determine 17 primary indexes (see Table A1), we not only refer to the relevant specifications of open pit mine but also add to concern factors for high slope stability by technical and managerial personnel of the open pit mine.

The parameter sets of risk assessment are

$$A = \{B_1, B_2, B_3, B_4\} \tag{16}$$

where B_1 is hydrological-climatic conditions, and B_2 is internal geological structure of slope. B_3 and B_4 are slope geometry and inducing factors of landslide, respectively.

$$B_1 = \{e_{11}, e_{12}, e_{13}, e_{14}\} \tag{17}$$

$$B_2 = \{e_{21}, e_{22}, e_{23}, e_{24}, e_{25}\} \tag{18}$$

$$B_3 = \{e_{31}, e_{32}, e_{33}, e_{34}\} \tag{19}$$

$$B_4 = \{e_{41}, e_{42}, e_{43}, e_{44}\} \tag{20}$$

where e_{11} is weathering and freeze-thaw, and e_{12} is the state of groundwater. e_{13} is permeability of rock and soil layer, and e_{14} is annual rainfall. e_{21} and e_{22} are lithology and geological structure, respectively. e_{23} and e_{24} are slope structure and internal friction angle, respectively. e_{25} is cohesion of slope. e_{31} and e_{32} are slope angle and slope height, respectively. e_{33} is relationship between soft surface and slope surface, and e_{34} is slope morphology. e_{41} and e_{42} are human factors and impact of blasting, respectively. e_{43} and e_{44} are slope angle of excavation and earthquake intensity, respectively. $B_1 \sim B_4$ are primary indicators and $e_{11} \sim e_{44}$ are secondary indicators.

The slope risk evaluation result set is

$$X = \{x_1, x_2, \dots, x_n\} \tag{21}$$

where n is the number of evaluation grades.

3.1. Determining the Weights in Different Time Range

If $s = [(a^-, a^+); b; c; (d^-, d^+)]$ is the interval trapezoidal fuzzy number, its entropy value is

$$E(s) = \left| \frac{1}{4} \left(\frac{a^- + a^+}{2} + b + c + \frac{d^- + d^+}{2} \right) - 0.5 \right| \tag{22}$$

The entropy matrix of $E_{B_q}^k = (E_{B_q}^k(e_{ij}^{(k)}))_{m \times n}$ at a different range is obtained by calculating the values of B_1, B_2, B_3 using Equation (22). $(e_{ij}^{(k)})_{n \times m}$ is the k th evaluation matrix. $e_{ij}^{(k)} (i = 1, 2, 3 \dots n; j = 1, 2, 3 \dots m)$ is the value of attribute c_j in the form of interval trapezoidal fuzzy number about evaluation grade t_i at time point of t_k .

Where $i = 1, 2, 3; k = 1, 2 \dots; j = q1, q2 \dots ql; q = 1, 2, 3, 4$. ql represents the number of parameters of the index B_q . Then, all the entropy values in the corresponding entropy matrix are added.

The entropy matrix can be obtained

$$E(B_q^k) = \frac{1}{mn} \sum_{i=1}^m \sum_{j=1}^n E(e_{ij}^{(k)}) \tag{23}$$

The corresponding weight $w(B_q^k)$ at the moment t_k of B_q

$$w(B_q^k) = \frac{1 - E(B_q^k)}{\sum_{i=1}^m (1 - E(B_q^k))} \tag{24}$$

3.2. Determining the Index Weight by FAHP Method

In order to determine the weight of each influencing factor, FAHP [44–46] method is used and a fuzzy consistent matrix is firstly constructed, and the matrix $A = (a_{ij})_{n \times n}$ satisfies the following conditions:

$$\begin{cases} 0 \leq a_{ij} \leq 1 (i, j = 1, 2, 3 \dots, n) \\ a_{ij} + a_{ji} = 1 (i, j = 1, 2, 3 \dots, n) \\ \forall i, j, a_{ij} = \omega_i - \omega_j + 0.5 \end{cases} \tag{25}$$

If A is a fuzzy consistent matrix, the weight ω can be denoted by

$$\omega_i = \frac{1}{n} \left(\sum_{j=1}^n a_{ij} + 1 - \frac{n}{2} \right) \tag{26}$$

It is worth noting that when $\sum_{j=1}^n a_{ij} \leq \frac{n}{2} - 1$, it needs to be modified until $\omega_i \geq 0$ is satisfied.

3.3. Integration and Decision Method of Interval Trapezoidal Fuzzy Soft Sets

Let $U = \{x_1, x_2, \dots, x_m\}$ be an initial universe set and $A = \{e_1, e_2, \dots, e_n\}$ be a set of parameters. The matrix of $\tilde{F}_k = (S_{F_k(e_j)}(x_i))_{m \times n}$ is corresponding to the interval trapezoidal fuzzy soft set of (F_k, A) . Where, $i = 1, 2, \dots, m; j = 1, 2, \dots, n; k = 1, 2, \dots, K$. $S_{F_k(e_j)}(x_i)$ is the corresponding interval trapezoidal fuzzy number of $F_k(e_j)$ and x_i , the interval trapezoidal fuzzy soft matrix between the algorithm is given as follows.

If $\tilde{F}_1 = (S_{F_1(e_j)}(x_i))_{m \times n}$ and $\tilde{F}_2 = (S_{F_2(e_j)}(x_i))_{m \times n}$ are interval trapezoidal fuzzy soft matrix, and $c > 0$, we can obtain

$$\tilde{F}_1 + \tilde{F}_2 = (S_{F_1(e_j)}(x_i))_{m \times n} + (S_{F_2(e_j)}(x_i))_{m \times n} \tag{27}$$

$$c\tilde{F}_1 = (cS_{F_1(e_j)}(x_i))_{m \times n} \tag{28}$$

If $\tilde{F}_k (k = 1, 2, \dots, K)$ is the interval trapezoidal fuzzy soft matrix and the weight satisfies the conditions of $\omega \in [0, 1]$ and $\sum_{k=1}^K \omega_k = 1$.

The weighted average operator of the interval trapezoidal fuzzy matrix can be denoted by

$$f_\omega(\tilde{F}_1, \tilde{F}_2, \dots, \tilde{F}_K) = \sum_{k=1}^K \omega_k \tilde{F}_k \tag{29}$$

We can obtain

$$f_\omega(\tilde{F}_1, \tilde{F}_2, \dots, \tilde{F}_K) = \sum_{k=1}^K (\omega_k S_{\tilde{F}_k(e_j)}(x_i))_{m \times n} \tag{30}$$

The integrated synthetic interval trapezoidal fuzzy soft matrix of $\tilde{F}_K (k = 1, 2, \dots, K)$ is denoted as $\tilde{R} = (r_{ij})_{m \times n}$.

The decision values are used to deal with the decision problems of the interval trapezoidal fuzzy soft sets, and the decision values for x_i in the universe set based on interval trapezoidal fuzzy soft sets in the domain are denoted by

$$\eta_i = \sum_{j=1}^m ((\tau_i^- - \tau_j^-) + (\tau_i^+ - \tau_j^+) + (\varphi_i - \varphi_j) + (\varepsilon_i - \varepsilon_j) + (\gamma_i^- - \gamma_j^-) + (\gamma_i^+ - \gamma_j^+)) \tag{31}$$

where the corresponding interval trapezoidal fuzzy number of x_i is

$$S(x_i) = [(\tau_i^-, \tau_i^+); \varphi_i; \varepsilon_i, (\gamma_i^-, \gamma_i^+)] \tag{32}$$

3.4. Case Study

3.4.1. Dynamic Risk Assessment Based on Trapezoidal Fuzzy Soft Set in Shengli Open-Pit Mine

(1) Decision-making steps and methods

Based on above interval trapezoidal fuzzy soft set model of high slope in an open-pit coal mine, the dynamic evaluation risk steps of high slope in an open-pit coal mine are divided into four steps:

- (1) Determine the times when the risk factors affecting the slope stability of open-pit mine are strong superimposed;
- (2) Determine the weight of each parameter using Equations (22)–(26);
- (3) Integrate interval trapezoidal fuzzy soft matrix at different times using Equation (30);
- (4) Calculate the decision values corresponding to different risks using Equation (31).

The multi-attribute decision integration and evaluation of all risk factor parameters in all time periods are carried out by dynamic interval trapezoidal fuzzy soft sets.

- (2) Determination of values for dynamic model parameter set

The north end slope of Shengli #1 open-pit mine is taken in this case study (see Figure 2). The slope height and maximum slope angle are, respectively, 200 m and 57° . Three moments were selected, i.e., $T = \{t_1, t_2, t_3\}$, t_1 is 1 July 2016; t_2 is 1 August 2016 and t_3 is 1 September 2016. The three time points (July, August and September) selected are the times with strong superposition of risk factors for open-pit mine slope. In this time period, there are many unstable factors inducing landslides. On the one hand, these three months are the rainy season for the open-pit mines in northern China, with a relatively concentrated and large rainfall, and the slope stability is greatly affected by hydrogeological factors. On the other hand, the open-pit mines in northern China can only be mined but not stripped in winter due to weather reasons. In order to leave enough earthwork and coal for winter mining, the blasting frequency during the three months (July, August and September) is relatively large, and the slope stability is greatly affected by mining factors. The risk decision of high slope in open-pit mine is evaluated from four primary risk factors (S), the hydrological and climatic conditions (B_1), the slope internal geological structure (B_2), the slope geometric conditions (B_3), and landslide risk factors (B_4). The risk level may be labeled as low, general and high, which are denoted by (x_1), (x_2), and (x_3), respectively. In addition, 17 secondary indicators are selected to carry out risk assessment in four primary indicators. This will be described in the third part later on. The risk grade is divided by considering the influence of comprehensive factors. Low and medium are classified as low decision risk, high as general decision risk, and dangerous and extremely dangerous as high decision risk. The expert evaluation method was used to evaluate the slope risk factors of open-pit mine. Data were collected mainly through questionnaires. A sample of the questionnaire is attached. The data were mainly collected from the production technicians, stripping workers and management personnel of Shengli Open-pit coal mine. It covers all positions of frontline production, management and technology in open-pit coal mines. Among them, 80 questionnaires were sent out by Shengli open-pit coal mine, and 72 questionnaires were effectively recovered. The parameters of slope risk factor B_1 , B_2 , B_3 and B_4 at time t_1 , t_2 and t_3 are listed in Tables A2–A12 in Appendix A.

- (3) Calculation of weights for dynamic model



Figure 2. High slopes of Shengli #1 open-pit mine.

The values of the four primary risk indicators of B_1 , B_2 , B_3 and B_4 are calculated by Equation (22), subsequently the entropy matrix of $E_{B_q}^k = (E_{ij}^{(k)})_{m \times n}$ corresponding to t_k

at different moments can be obtained. For example, the calculation results of the entropy matrix of B_1 at different times are shown in Tables 1–3.

Table 1. Entropy of each parameter of hydrological and climatic conditions B_1 at time t_1 .

	$E(e_{11})$	$E(e_{12})$	$E(e_{13})$	$E(e_{14})$
x_1	0.13	0.15	0.13	0.15
x_2	0.15	0.05	0.21	0.06
x_3	0.04	0.08	0.04	0.20

Table 2. Entropy of each parameter of hydrological and climatic conditions B_1 at time t_2 .

	$E(e_{11})$	$E(e_{12})$	$E(e_{13})$	$E(e_{14})$
x_1	0.06	0.20	0.13	0.05
x_2	0.18	0.14	0.23	0.08
x_3	0.06	0.08	0.14	0.23

Table 3. Entropy of each parameter of hydrological and climatic conditions B_1 at time t_3 .

	$E(e_{11})$	$E(e_{12})$	$E(e_{13})$	$E(e_{14})$
x_1	0.21	0.28	0.10	0.10
x_2	0.10	0.10	0.29	0.16
x_3	0.15	0.08	0.15	0.08

The weight of B_1 is calculated by Equations (23) and (24), and the result is

$$w_{B_1} = (0.219, 0.395, 0.386) \quad (33)$$

Similarly, the weights of B_2 , B_3 and B_4 can be obtained

$$w_{B_2} = (0.214, 0.396, 0.390) \quad (34)$$

$$w_{B_3} = (0.229, 0.394, 0.377) \quad (35)$$

$$w_{B_4} = (0.235, 0.385, 0.380) \quad (36)$$

3.4.2. Risk Evaluation

Based on the above interval valued fuzzy set model, the dynamic risk of the north end slope in Shengli #1 open-pit coalmine is evaluated comprehensively. The above three time points are selected to evaluate the risk from four aspects, i.e., hydro-climatic conditions, slope internal geological structure, slope geometric conditions and induced factors. The risk evaluation of high slope is divided into three levels: low (x_1), general (x_2) and high (x_3). Combined with the above theory, the weights at different times are obtained and then the comprehensive interval trapezoidal fuzzy soft set evaluation information for different parameter sets in all time range can be obtained by Equation (29). That is, the comprehensive evaluation values of influencing factors B_1 , B_2 , B_3 and B_4 in the whole time range subjected to different risks can be obtained as listed in Tables A14–A17 in Appendix A.

Meanwhile, the fuzzy symmetry matrix of each parameter for the risk factors (i.e., hydro-climatic conditions, internal geological structure, geometric conditions and induced factors) are obtained by FAHP theory in Tables A18–A21, as shown in Appendix A. The corresponding weight vectors are calculated as follows

$$w_{B_1} = (0.225, 0.250, 0.250, 0.275) \quad (37)$$

$$w_{B_2} = (0.160, 0.260, 0.220, 0.180, 0.180) \quad (38)$$

$$w_{B_3} = (0.150, 0.250, 0.250, 0.350) \quad (39)$$

$$w_{B_4} = (0.225, 0.375, 0.300, 0.100) \quad (40)$$

The fuzzy symmetric matrix for primary risk indicators is obtained in Table A22 in Appendix A. The weight value is obtained by Equation (41)

$$\omega_A = (0.150, 0.150, 0.325, 0.375) \quad (41)$$

The weights of risk parameters for the risk evaluation system of high slope in open-pit mine are given in Table 4.

Table 4. Weights of risk parameters for the risk evaluation system.

Primary Indicator	Parameters	Primary Weight	Parameter Weights
Hydro-climatic conditions	Weathering and freeze-thaw	0.150	0.225
	Groundwater occurrence		0.250
	Water permeability		0.250
	Average annual rainfall		0.275
Geological structure inside the slope	Lithology	0.150	0.160
	Geological structure		0.260
	Slope structure		0.220
	Internal friction		0.180
	Cohesion		0.180
Slope geometric conditions	Slope angle	0.325	0.150
	Slope height		0.250
	Relationship between weak surface (fault) and slope		0.250
	Slope morphology		0.350
Induced factors	Human factors	0.375	0.225
	Destructive factor		0.375
	Excavation angle		0.300
	Seismic intensity		0.100

The interval trapezoidal fuzzy soft set of different parameters are integrated by Equation (30). The integrated evaluation value of different parameters belonging to open-pit slope risk and the integrated value of surface mine slope risk relative to different risk grades are obtained in Tables A23 and A24 in Appendix A.

The comprehensive evaluation value of the relative risk level, which is either low, general or high, can be obtained. The evaluation value which represents low risk for high slope in Shengli open-pit mine is

$$\mu_1 = [(0.225, 0.401); 0.427; 0.491; (0.548, 0.704)] \quad (42)$$

The evaluation value which represents general risk for high slope is

$$\mu_2 = [(0.243, 0.408); 0.414; 0.481; (0.546, 0.699)] \quad (43)$$

The evaluation value which represents high risk for high slope is

$$\mu_3 = [(0.295, 0.434); 0.450; 0.512; (0.567, 0.681)] \quad (44)$$

Further, the decision value of the high slope risk in the open-pit which is subject to low risk, general risk, and higher risk can be obtained. The integrated evaluation value is calculated according to Equation (28). The results are shown in Table 5.

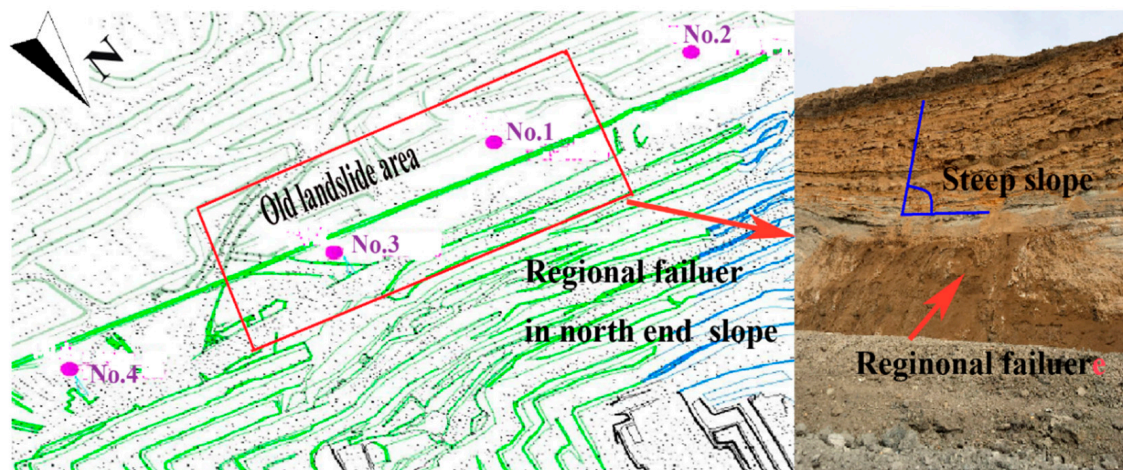
Table 5. Different decision factors relative to open-pit slope risk.

	B_1	B_2	B_3	B_4
η_1	0.336	−0.446	−0.156	−0.185
η_2	−1.257	0.397	−1.098	0.88
η_3	0.921	0.049	1.254	−0.695

As shown in Table 5, for the decision-making results of the high slope in Shengli #1 open-pit mine, the values of B_1 and B_3 indicate a high risk level, while the values of B_2 and B_4 indicate a general risk level. Thus, among the many factors affecting the instability of the slope of Shengli #1 open-pit coal mine, hydro-climatic conditions and slope geometric conditions belong to high risk factors. Special attention should be paid to hydrology and slope geometry during slope stability maintenance. For example, slope reinforcement and radar displacement monitoring should be planned and performed during the rainy season. The stability evaluation should be performed when designing the slope angle.

4. Verification with Field Data

In order to verify the rationality of the above-mentioned risk evaluation method, the in-situ monitoring data were analyzed in the north end slope of Shengli #1 coalmine. The anchor monitoring points are arranged to monitor the axial force variation of the anchor cable and the displacement parameters are analyzed in the north end of the slope. Field layout with 4 anchor monitoring points and regional failure of a certain landslide in the north end slope is shown in Figure 3. The correlation laws were obtained by field monitoring results of the slope sliding in the north end slope of the open-pit mine in 2016, the axial force variation of the anchor cable in 2016, the rainfall in 2016 and the displacement of the north slope of the slope. The GPS monitoring displacements before and after the landslide accident are presented in Figure 4. The axial force variation of the anchor cable of the north end slope in 2016 are presented in Figure 5, and the rainfall and the displacement of the north side in 2017 are presented in Figure 6.

**Figure 3.** Field layout with 4 anchor monitoring points and regional landslide in north end slope.

The maximum angles of 975–1015 level and 915–945 level in the north end slope are 45° and 57° , respectively. It can be seen from Figures 4–6 that the slope of displacement curve started to be relatively flat, then increased first and then decreased, and finally the slope gradually restored stability from June 16 to June 30. The maximum horizontal displacement of 915–945 level is 210 mm and that of 975–1015 level is 190 mm. Meanwhile, the horizontal displacement of 915–945 level (larger angle) is larger than that of 975–1015 level (smaller angle). The average angle of the north slope is larger than that of the southern slope. Historical data show that the frequency of landslides in the north slope is higher than in

the southern slope, so the geometric angle of the slope has a greater impact on the stability of the slope. In March and June, 2016, the anchor cable axial force suddenly increased, and the maximum change occurred at the monitoring points of No. 1 and No. 3 which are located in the old landslide area. The above results indicate that the high slope has a potential landslide risk. The horizontal displacement and settlement of the slope in 2016 are much larger in the rainy season than in other months, which indicates that the precipitation conditions have a greater impact on the stability of the slope. The above statistical results are consistent with the risk evaluation results of the interval trapezoidal fuzzy soft set proposed in this work.

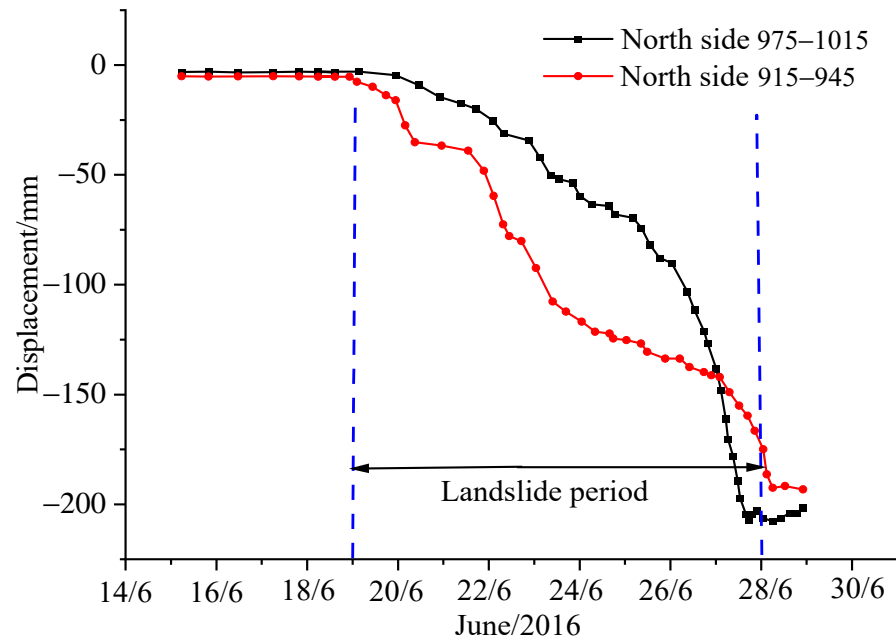


Figure 4. Displacement curves of the north end slope from 16 June to 29 June 2016.

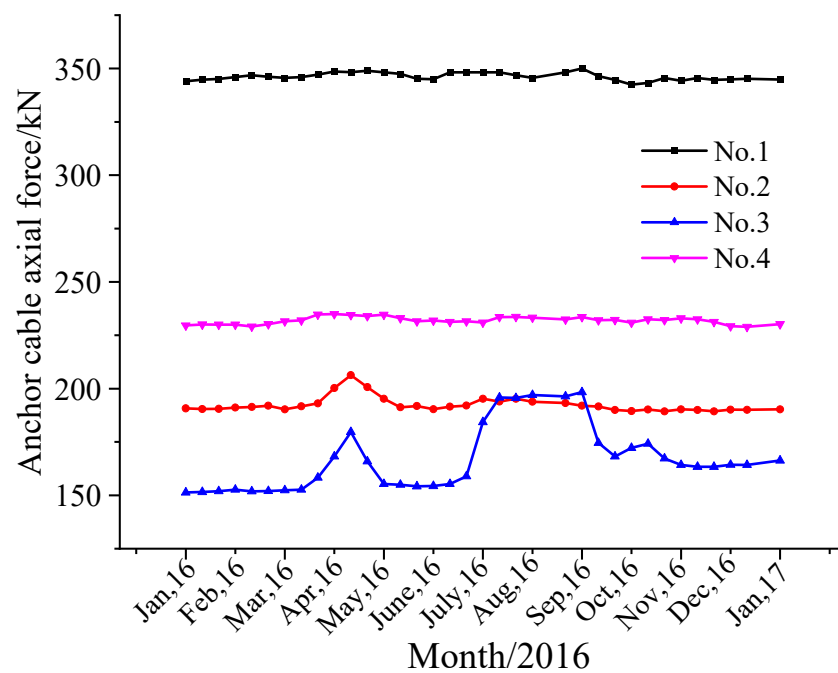


Figure 5. Axial force variation of anchor cable for the north end slope in 2016.

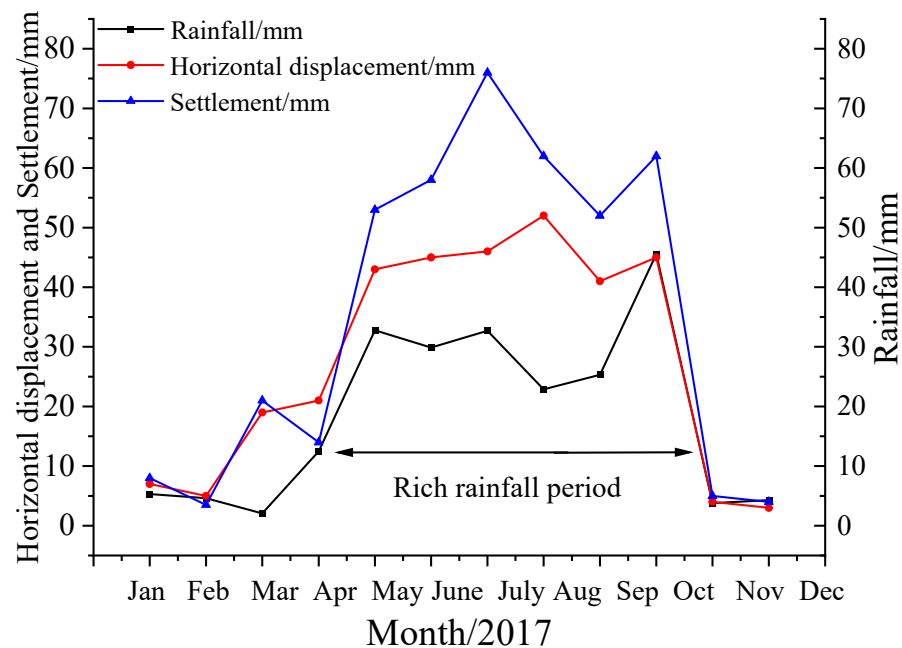


Figure 6. Rainfall and displacement curves of the north end slope in 2017.

5. Conclusions

A dynamic risk assessment method of high slope in open-pit coalmine based on interval trapezoidal fuzzy soft set has been proposed for realizing dynamic early warning of high slope risk in open-pit coalmine. The proposed dynamic interval trapezoidal fuzzy soft set method integrates time points and the weights of slope risk factors. The formulations of the proposed method are derived, along with a detailed introduction to the procedures for implementation. Finally, the method is illustrated by a case study of high slope in Shengli #1 open mine located in Xilinhot, Inner Mongolia to verify the effectiveness of the proposed method. The main conclusions are summarized as follows:

- (1) The proposed method can effectively describe dynamic evaluation information of high slope, which makes it clear for the correlation between the influence of various uncertain factors on the slope and the time dimension. Compared with the traditional probabilistic analytical method, the proposed method can integrate time points and the weights of slope risk factors, especially for complex high slopes in open-pit coalmine, which enhances the practicability of interval trapezoidal fuzzy soft set theory in slope reliability analysis;
- (2) The risk dynamic evaluation model of high slope in an open-pit coal mine is established based on developed interval trapezoidal fuzzy soft set. In the model, the integration operator of interval trapezoidal fuzzy soft set is calculated and the comprehensive interval trapezoidal fuzzy soft set evaluation information in all time periods for different parameter sets can be obtained. The risk assessment of different factors with time can be easily achieved with the proposed method. This is not achievable by the traditional probabilistic analyses, which greatly facilitate the application of the interval trapezoidal fuzzy soft set method in probabilistic slope stability analysis;
- (3) The dynamic risk assessment model established above is applied in a case study for the north end slope of Shengli #1 open-pit mine. In the application of the model, three time points are selected to calculate the parameter values required by the above method, and 17 secondary risk factors of the high slope at different time points are evaluated. The results show that, for the north end slope stability of Shengli #1 open-pit coal mine, the risks of hydro-climatic conditions and slope geometric conditions are relatively high, and the risks of internal geological structure and induced factors of slope are general. Meanwhile, the field monitoring parameters of the north end slope

at different time ranges are analyzed; the results show that the above-mentioned slope dynamic evaluation model and method are reasonable and effective. In the process of slope reinforcement at the later stage for Shengli #1 open-pit mine, the influence of hydrological and climatic conditions and geometric shapes should be evaluated.

Author Contributions: Conceptualization, Z.W., M.H. and P.Z.; methodology, Z.W. and P.Z.; software, M.H.; validation, X.L. and S.Y.; formal analysis, Z.W.; investigation, P.Z., X.L. and S.Y.; data curation, P.Z.; writing—original draft preparation, Z.W., M.H. and P.Z.; writing—review and editing, Z.W.; funding acquisition, Z.W. and X.L. All authors have read and agreed to the published version of the manuscript.

Funding: This research was funded by Scientific and Technological Project of Henan Province (222102320060), Strength Improvement Plan of the Advantageous Disciplines of Zhongyuan University of Technology (SD202232), Henan Postgraduate Education Reform and Quality Improvement Project (YIS2022SZ16), Postgraduate Education Reform and Quality Improvement Project of Zhongyuan University of Technology (JG202220).

Institutional Review Board Statement: Not applicable.

Informed Consent Statement: Not applicable.

Data Availability Statement: Not applicable.

Conflicts of Interest: The authors declare no conflict of interest.

Appendix A

Table A1. Risk assessment index system and classification standard for slope of open-pit coal mine.

Primary Indicator	Secondary Indicators	LEVEL OF RISK				
		Low	Medium	High	Dangerous	Extremely Dangerous
Hydro-climatic conditions	Weathering and freeze-thaw	Tiny	Low	Medium	large	strong
	Groundwater occurrence	Tiny	Low	Medium	large	strong
	Water permeability	Tiny	Low	Medium	large	strong
Average annual rainfall		<200	200~400	400~700	700~1100	>1100
Geological structure inside the slope	Lithology	Wholly	Slightly weathered	Weakly weathered	Cracked	Granular structures
	Geological structure	Simple	relatively simple	Generally	Relatively complex	Complex
	Slope structure	Overall structure	Blocky structure	Layered structure	Cataclastic structure	Granular Structures
	Internal friction	>35	35~28	28~21	21~14	<14
	Cohesion	>220	120~220	80~120	50~80	<50
Slope geometric conditions	Slope angle	<20	20~30	30~40	40~50	>50
	Slope height	<30	30~60	60~100	100~200	>200
	Relationship between weak surface (fault) and slope	Perpendicular slope	Vertical slope	Transverse slope	Bedding slope	Parallel slope
	Slope morphology	Concave slope	Concave and straight mixing	Straight slope	Convex and straight mixing	Convex slope
Induced factors	Human factors	Tiny	Low	Medium	Large	Strong
	Destructive factor	Tiny	Low	Medium	Large	Strong
	Excavation angle	<15	15~30	30~45	45~60	>60
	Seismic intensity	<3	3~5	5~7	7~8	>8

Table A2. The different risk evaluation values subordinated by influencing factors of B_1 at time t_1 .

	e_{11}	e_{12}	e_{13}	e_{14}
x_1	[(0.2,0.3);0.3; 0.4;(0.5,0.6)]	[(0.2,0.3);0.3; 0.4;(0.4,0.5)]	[(0.4,0.5);0.6; 0.7;(0.7,0.8)]	[(0.5,0.6);0.6; 0.7;(0.7,0.8)]
x_2	[(0.2,0.3);0.3; 0.4;(0.4,0.5)]	[(0.3,0.4);0.5; 0.6;(0.7,0.8)]	[(0.5,0.7);0.7; 0.7;(0.8,0.9)]	[(0.2,0.3);0.3; 0.4;(0.5,0.6)]
x_3	[(0.3,0.5);0.5; 0.6;(0.6,0.7)]	[(0.3,0.4);0.4; 0.4;(0.5,0.6)]	[(0.3,0.5);0.5; 0.6;(0.6,0.7)]	[(0.5,0.6);0.7; 0.7;(0.8,0.9)]

Table A3. The different risk evaluation values subordinated by influencing factors of B_2 at time t_1 .

	e_{21}	e_{22}	e_{23}	e_{24}	e_{25}
x_1	[(0.5,0.6);0.7; 0.7;(0.8,0.9)]	[(0.2,0.3);0.4; 0.4;(0.5,0.6)]	[(0.5,0.6);0.7; 0.7;(0.8,0.9)]	[(0.3,0.4);0.4; 0.4;(0.5,0.6)]	[(0.3,0.4);0.4; 0.4;(0.5,0.6)]
x_2	[(0.1,0.3);0.3; 0.3;(0.4,0.5)]	[(0.5,0.6);0.7; 0.7;(0.8,0.9)]	[(0.6,0.7);0.7; 0.7;(0.8,0.9)]	[(0.3,0.4);0.5; 0.6;(0.7,0.8)]	[(0.2,0.3);0.3; 0.4;(0.4,0.5)]
x_3	[(0.3,0.5);0.5; 0.6;(0.6,0.7)]	[(0.2,0.3);0.4; 0.4;(0.5,0.6)]	[(0.3,0.5);0.5; 0.6;(0.6,0.7)]	[(0.6,0.7);0.7; 0.7;(0.8,0.9)]	[(0.2,0.4);0.4; 0.4;(0.5,0.6)]

Table A4. The different risk evaluation values subordinated by influencing factors of B_3 at time t_1 .

	e_{31}	e_{32}	e_{33}	e_{34}
x_1	[(0.4,0.5);0.6; 0.7;(0.7,0.8)]	[(0.5,0.6);0.7; 0.7;(0.8,0.9)]	[(0.2,0.3);0.3; 0.4;(0.4,0.5)]	[(0.1,0.2);0.2; 0.3;(0.3,0.4)]
x_2	[(0.2,0.3);0.4; 0.4;(0.5,0.6)]	[(0.3,0.5);0.5; 0.6;(0.6,0.7)]	[(0.5,0.6);0.6; 0.7;(0.8,0.9)]	[(0.1,0.3);0.3; 0.4;(0.4,0.5)]
x_3	[(0.1,0.3);0.3; 0.4;(0.4,0.5)]	[(0.2,0.4);0.4; 0.4;(0.5,0.6)]	[(0.4,0.5);0.6; 0.7;(0.7,0.8)]	[(0.5,0.6);0.7; 0.7;(0.8,0.9)]

Table A5. The different risk evaluation values subordinated by influencing factors of B_4 at time t_1 .

	e_{41}	e_{42}	e_{43}	e_{44}
x_1	[(0.2,0.3);0.3; 0.4;(0.4,0.5)]	[(0.2,0.4);0.4; 0.4;(0.5,0.6)]	[(0.1,0.2);0.2; 0.3;(0.3,0.4)]	[(0.4,0.5);0.6; 0.7;(0.7,0.8)]
x_2	[(0.4,0.6);0.6; 0.7;(0.7,0.8)]	[(0.2,0.3);0.3; 0.4;(0.5,0.6)]	[(0.3,0.4);0.4; 0.4;(0.5,0.6)]	[(0.6,0.7);0.7; 0.8;(0.9,1)]
x_3	[(0.1,0.4);0.4; 0.4;(0.5,0.6)]	[(0.1,0.3);0.3; 0.3;(0.4,0.5)]	[(0.3,0.5);0.5; 0.6;(0.6,0.7)]	[(0.5,0.7);0.7; 0.7;(0.8,0.9)]

Table A6. The different risk evaluation values subordinated by influencing factors of B_1 at time t_2 .

	e_{11}	e_{12}	e_{13}	e_{14}
x_1	[(0.3,0.4);0.4; 0.4;(0.5,0.7)]	[(0.5,0.6);0.7; 0.7;(0.8,0.9)]	[(0.2,0.3);0.3; 0.4;(0.5,0.6)]	[(0.4,0.5);0.5; 0.6;(0.6,0.7)]
x_2	[(0.1,0.2);0.2; 0.4;(0.5,0.6)]	[(0.4,0.6);0.6; 0.7;(0.7,0.8)]	[(0.1,0.2);0.2; 0.3;(0.4,0.5)]	[(0.3,0.4);0.4; 0.4;(0.5,0.6)]
x_3	[(0.3,0.5);0.5; 0.6;(0.7,0.8)]	[(0.4,0.5);0.5; 0.6;(0.7,0.8)]	[(0.4,0.6);0.6; 0.7;(0.7,0.8)]	[(0.5,0.6);0.7; 0.8;(0.8,0.9)]

Table A7. The different risk evaluation values subordinated by influencing factors of B_2 at time t_2 .

	e_{21}	e_{22}	e_{23}	e_{24}	e_{25}
x_1	[(0.2,0.3);0.4; 0.4;(0.5,0.6)]	[(0.1,0.2);0.2; 0.3;(0.4,0.5)]	[(0.3,0.6);0.6; 0.7;(0.8,0.9)]	[(0.4,0.6);0.6; 0.7;(0.8,0.9)]	[(0.3,0.4);0.4; 0.4;(0.6,0.7)]
x_2	[(0.3,0.5);0.5; 0.6;(0.7,0.8)]	[(0.1,0.3);0.3; 0.4;(0.4,0.6)]	[(0.5,0.7);0.7; 0.7;(0.8,0.9)]	[(0.1,0.3);0.3; 0.4;(0.5,0.6)]	[(0.2,0.3);0.3; 0.4;(0.4,0.5)]
x_3	[(0.4,0.5);0.6; 0.7;(0.7,0.8)]	[(0.2,0.4);0.4; 0.4;(0.5,0.7)]	[(0.3,0.5);0.5; 0.6;(0.7,0.8)]	[(0.5,0.7);0.7; 0.7;(0.8,0.9)]	[(0.4,0.5);0.5; 0.6;(0.6,0.7)]

Table A8. The different risk evaluation values subordinated by influencing factors of B_3 at time t_2 .

	e_{31}	e_{32}	e_{33}	e_{34}
x_1	[(0.2,0.4);0.4; 0.4;(0.5,0.6)]	[(0.5,0.6);0.7; 0.7;(0.8,0.9)]	[(0.1,0.2);0.3; 0.4;(0.4,0.5)]	[(0.3,0.5);0.5; 0.6;(0.7,0.8)]
x_2	[(0.2,0.3);0.3; 0.4;(0.5,0.6)]	[(0.5,0.6);0.6; 0.7;(0.7,0.8)]	[(0.1,0.2);0.2; 0.3;(0.3,0.4)]	[(0.3,0.4);0.4; 0.4;(0.5,0.6)]
x_3	[(0.3,0.5);0.5; 0.6;(0.7,0.8)]	[(0.4,0.5);0.5; 0.6;(0.7,0.8)]	[(0.4,0.6);0.6; 0.7;(0.8,0.9)]	[(0.5,0.6);0.7; 0.8;(0.8,0.9)]

Table A9. The different risk evaluation values subordinated by influencing factors of B_4 at time t_2 .

	e_{41}	e_{42}	e_{43}	e_{44}
x_1	[(0.3,0.5);0.5; 0.6;(0.7,0.8)]	[(0.3,0.5);0.6; 0.7;(0.7,0.8)]	[(0.1,0.2);0.2; 0.3;(0.3,0.4)]	[(0.4,0.5);0.5; 0.6;(0.9,1)]
x_2	[(0.1,0.3);0.3; 0.4;(0.5,0.6)]	[(0.6,0.7);0.7; 0.8;(0.9,1)]	[(0.2,0.3);0.3; 0.4;(0.5,0.6)]	[(0.4,0.5);0.6; 0.7;(0.8,0.9)]
x_3	[(0.2,0.4);0.4; 0.4;(0.6,0.7)]	[(0.1,0.3);0.3; 0.4;(0.4,0.6)]	[(0.1,0.2);0.2; 0.2;(0.3,0.4)]	[(0.1,0.3);0.3; 0.4;(0.5,0.6)]

Table A10. The different risk evaluation values subordinated by influencing factors of B_1 at time t_3 .

	e_{11}	e_{12}	e_{13}	e_{14}
x_1	[(0.5,0.7);0.7; 0.7;(0.8,0.9)]	[(0.1,0.2);0.2; 0.2;(0.2,0.5)]	[(0.1,0.4);0.4; 0.4;(0.5,0.6)]	[(0.1,0.6);0.6; 0.7;(0.7,0.8)]
x_2	[(0.1,0.4);0.4; 0.4;(0.5,0.6)]	[(0.1,0.6);0.6; 0.7;(0.7,0.8)]	[(0.1,0.2);0.2; 0.2;(0.2,0.4)]	[(0.1,0.3);0.3; 0.4;(0.4,0.5)]
x_3	[(0.2,0.3);0.3; 0.4;(0.4,0.5)]	[(0.3,0.4);0.4; 0.4;(0.5,0.6)]	[(0.5,0.6);0.6; 0.7;(0.7,0.8)]	[(0.3,0.4);0.4; 0.4;(0.5,0.6)]

Table A11. The different risk evaluation values subordinated by influencing factors of B_2 at time t_3 .

	e_{21}	e_{22}	e_{23}	e_{24}	e_{25}
x_1	[(0.1,0.7);0.7; 0.7;(0.8,0.9)]	[(0.1,0.4);0.4; 0.4;(0.5,0.6)]	[(0.1,0.2);0.2; 0.3;(0.3,0.5)]	[(0.1,0.6);0.6; 0.7;(0.7,0.8)]	[(0.1,0.3);0.3; 0.4;(0.4,0.5)]
x_2	[(0.1,0.6);0.6; 0.7;(0.7,0.8)]	[(0.1,0.3);0.3; 0.4;(0.5,0.6)]	[(0.1,0.4);0.4; 0.4;(0.5,0.6)]	[(0.1,0.7);0.7; 0.8;(0.9,1)]	[(0.5,0.6);0.6; 0.7;(0.7,0.8)]
x_3	[(0.3,0.4);0.4; 0.4;(0.5,0.6)]	[(0.1,0.2);0.2; 0.3;(0.3,0.4)]	[(0.4,0.5);0.5; 0.6;(0.6,0.7)]	[(0.6,0.7);0.7; 0.7;(0.8,0.9)]	[(0.3,0.4);0.4; 0.4;(0.5,0.6)]

Table A12. The different risk evaluation values subordinated by influencing factors of B_3 at time t_3 .

	e_{31}	e_{32}	e_{33}	e_{34}
x_1	[(0.1,0.2);0.2; 0.2;(0.2,0.4)]	[(0.2,0.3);0.3; 0.4;(0.4,0.6)]	[(0.2,0.3);0.3; 0.3;(0.3,0.9)]	[(0.1,0.4);0.4; 0.4;(0.5,0.6)]
x_2	[(0.1,0.3);0.3; 0.3;(0.3,0.4)]	[(0.1,0.3);0.3; 0.4;(0.4,0.5)]	[(0.1,0.2);0.2; 0.2;(0.2,0.7)]	[(0.1,0.3);0.3; 0.3;(0.3,0.4)]
x_3	[(0.3,0.4);0.4; 0.4;(0.5,0.6)]	[(0.1,0.2);0.2; 0.2;(0.2,0.3)]	[(0.3,0.4);0.4; 0.4;(0.5,0.6)]	[(0.2,0.3);0.3; 0.4;(0.4,0.5)]

Table A13. The different risk evaluation values subordinated by influencing factors of B_4 at time t_3 .

	e_{41}	e_{42}	e_{43}	e_{44}
x_1	[(0.1,0.3);0.3; 0.4;(0.4,0.5)]	[(0.1,0.2);0.2; 0.2;(0.2,0.7)]	[(0.1,0.5);0.5; 0.6;(0.6,0.7)]	[(0.1,0.3);0.3; 0.3;(0.3,0.4)]
x_2	[(0.1,0.2);0.2; 0.2;(0.2,0.4)]	[(0.1,0.4);0.4; 0.4;(0.5,0.6)]	[(0.1,0.3);0.3; 0.3;(0.3,0.4)]	[(0.1,0.3);0.3; 0.4;(0.4,0.5)]
x_3	[(0.5,0.6);0.6; 0.7;(0.7,0.8)]	[(0.2,0.3);0.3; 0.4;(0.4,0.5)]	[(0.3,0.4);0.4; 0.4;(0.4,0.5)]	[(0.2,0.3);0.3; 0.3;(0.3,0.4)]

Table A14. The influencing factors of B_1 in the whole time period belong to the comprehensive evaluation value of different risks.

	e_{11}	e_{12}	e_{13}	e_{14}
x_1	[(0.37,0.53);0.53; 0.54;(0.65,0.79)]	[(0.30,0.41);0.47; 0.49;(0.57,0.74)]	[(0.21,0.39);0.42; 0.48;(0.55,0.66)]	[(0.33,0.56);0.56; 0.66;(0.66,0.77)]
x_2	[(0.12,0.30);0.30; 0.40;(0.48,0.58)]	[(0.27,0.56);0.58; 0.68;(0.70,0.80)]	[(0.21,0.35);0.35; 0.39;(0.47,0.62)]	[(0.21,0.34);0.34; 0.40;(0.46,0.56)]
x_3	[(0.26,0.43);0.43; 0.53;(0.58,0.69)]	[(0.34,0.44);0.44; 0.49;(0.59,0.70)]	[(0.42,0.56);0.56; 0.65;(0.66,0.77)]	[(0.43,0.53);0.61; 0.67;(0.72,0.83)]

Table A15. The influencing factors of B_2 in the whole time period belong to the comprehensive evaluation value of different risks.

	e_{21}	e_{22}	e_{23}	e_{24}	e_{25}
x_1	[(0.24,0.55);0.61; 0.61;(0.71,0.83)]	[(0.12,0.31);0.33; 0.36;(0.46,0.56)]	[(0.28,0.48);0.51; 0.58;(0.67,0.81)]	[(0.27,0.56);0.56; 0.65;(0.71,0.82)]	[(0.23,0.36);0.36; 0.4;(0.51,0.61)]
x_2	[(0.19,0.51);0.51; 0.60;(0.65,0.76)]	[(0.21,0.38);0.42; 0.48;(0.56,0.70)]	[(0.40,0.61);0.61; 0.61;(0.71,0.83)]	[(0.15,0.51);0.53; 0.64;(0.76,1)]	[(0.33,0.44);0.44; 0.54;(0.54,0.65)]
x_3	[(0.34,0.46);0.51; 0.58;(0.61,0.71)]	[(0.16,0.31);0.33; 0.36;(0.43,0.58)]	[(0.34,0.5);0.5; 0.6;(0.64,0.74)]	[(0.56,0.7);0.7; 0.7;(0.8,0.9)]	[(0.32,0.44);0.44; 0.49;(0.54,0.64)]

Table A16. The influencing factors of B_3 in the whole time period belong to the comprehensive evaluation value of different risks.

	e_{31}	e_{32}	e_{33}	e_{34}
x_1	[(0.22,0.36);0.39; 0.43;(0.47,0.6)]	[(0.4,0.51);0.59; 0.61;(0.7,0.83)]	[(0.16,0.26);0.3; 0.36;(0.36,0.73)]	[(0.18,0.4);0.4; 0.47;(0.56,0.67)]
x_2	[(0.16,0.3);0.32; 0.36;(0.43,0.53)]	[(0.33,0.48);0.48; 0.58;(0.58,0.69)]	[(0.21,0.32);0.32; 0.39;(0.45,0.69)]	[(0.18,0.34);0.34; 0.36;(0.41,0.51)]
x_3	[(0.26,0.42);0.42; 0.49;(0.57,0.68)]	[(0.25,0.38);0.38; 0.43;(0.51,0.62)]	[(0.36,0.51);0.53; 0.61;(0.69,0.8)]	[(0.4,0.51);0.59; 0.67;(0.7,0.82)]

Table A17. The influencing factors of B_4 in the whole time period belong to the comprehensive evaluation value of different risks.

	e_{41}	e_{42}	e_{43}	e_{44}
x_1	[(0.21,0.39);0.39; 0.49;(0.54,0.65)]	[(0.21,0.38);0.43; 0.49;(0.51,0.73)]	[(0.10,0.33);0.33; 0.43;(0.43,0.54)]	[(0.30,0.43);0.46; 0.54;(0.73,1.00)]
x_2	[(0.18,0.35);0.35; 0.43;(0.47,0.60)]	[(0.36,0.52);0.52; 0.61;(0.73,1.00)]	[(0.19,0.32);0.32; 0.36;(0.43,0.53)]	[(0.36,0.50);0.54; 0.65;(0.74,1.00)]
x_3	[(0.31,0.49);0.49; 0.54;(0.62,0.72)]	[(0.14,0.30);0.30; 0.38;(0.40,0.54)]	[(0.23,0.36);0.36; 0.39;(0.42,0.52)]	[(0.25,0.43);0.43; 0.46;(0.54,0.66)]

Table A18. Fuzzy symmetric matrix for influencing factors of hydrology-climate B_1 .

B_1	e_{11}	e_{12}	e_{13}	e_{14}
e_{11}	0.5	0.4	0.3	0.7
e_{12}	0.6	0.5	0.6	0.3
e_{13}	0.7	0.4	0.5	0.4
e_{14}	0.3	0.7	0.6	0.5

Table A19. Fuzzy symmetric matrix for influencing factors of geological structure in slope B_2 .

B_2	e_{21}	e_{22}	e_{23}	e_{24}	e_{25}
e_{21}	0.5	0.4	0.3	0.7	0.4
e_{22}	0.6	0.5	0.6	0.3	0.8
e_{23}	0.7	0.4	0.5	0.4	0.6
e_{24}	0.3	0.7	0.6	0.5	0.3
e_{25}	0.6	0.2	0.4	0.7	0.5

Table A20. Fuzzy symmetric matrix for influencing factors of slope geometry condition B_3 .

B_3	e_{31}	e_{32}	e_{33}	e_{34}
e_{31}	0.5	0.4	0.3	0.4
e_{32}	0.6	0.5	0.6	0.3
e_{33}	0.7	0.4	0.5	0.4
e_{34}	0.6	0.7	0.6	0.5

Table A21. Fuzzy symmetric matrix for inducing factors B_4 .

B_4	e_{41}	e_{42}	e_{43}	e_{44}
e_{41}	0.5	0.4	0.3	0.7
e_{42}	0.6	0.5	0.6	0.8
e_{43}	0.7	0.4	0.5	0.6
e_{44}	0.3	0.2	0.4	0.5

Table A22. Fuzzy symmetric matrix corresponding to first level index.

A	B_1	B_2	B_3	B_4
B_1	0.5	0.4	0.3	0.4
B_2	0.6	0.5	0.3	0.2
B_3	0.7	0.7	0.5	0.4
B_4	0.6	0.8	0.6	0.5

Table A23. The integrated evaluation value of different parameters belonging to open-pit slope risk.

	B_1	B_2	B_3	B_4
x_1	[(0.302,0.472);0.495; 0.548;(0.608,0.736)]	[(0.223,0.439);0.460; 0.509;(0.603,0.716)]	[(0.239,0.387);0.422; 0.473;(0.531,0.713)]	[(0.183,0.370);0.392; 0.476;(0.516,0.680)]
x_2	[(0.205,0.392);0.396; 0.467;(0.529,0.641)]	[(0.258,0.484);0.497; 0.568;(0.641,0.783)]	[(0.224,0.364);0.367; 0.426;(0.466,0.604)]	[(0.269,0.423);0.427; 0.498;(0.584,0.771)]
x_3	[(0.368,0.494);0.515; 0.588;(0.642,0.749)]	[(0.331,0.469);0.482; 0.533;(0.593,0.707)]	[(0.334,0.462);0.497; 0.567;(0.631,0.744)]	[(0.216,0.372);0.372; 0.426;(0.471,0.590)]

Table A24. Integrated value of surface mine slope risk relative to different risk grades.

	A
x_1	[(0.225,0.401);0.427;0.491;(0.548,0.704)]
x_2	[(0.243,0.408);0.414;0.481;(0.546,0.699)]
x_3	[(0.295,0.434);0.450;0.512;(0.567,0.681)]

References

- Whittall, J.R.; McDougall, S.; Eberhardt, E. A risk-based methodology for establishing landslide exclusion zones in operating open pit mines. *Int. J. Rock Mech. Min. Sci.* **2017**, *100*, 100–107. [[CrossRef](#)]
- Zhang, J.X.; Li, B.; Liu, Y.W.; Li, P.; Fu, J.W.; Chen, L.; Ding, P.C. Dynamic multifield coupling model of gas drainage and a new remedy method for borehole leakage. *Acta Geotech.* **2022**, *17*, 4699–4715. [[CrossRef](#)]
- Li, B.; Zhang, J.X.; Liu, Y.W.; Qu, L.N.; Liu, Q.; Sun, Y.X.; Xu, G. Interfacial porosity model and modification mechanism of broken coal grouting: A theoretical and experimental study. *Surf. Interfaces* **2022**, *33*, 102286. [[CrossRef](#)]

4. Nie, L.; Li, Z.C.; Zhang, M. Deformation character and stability analysis of the landslide caused by the mining activity: A case study in the west open-pit mine, China. *J. Balk. Tribol. Assoc.* **2016**, *22*, 1001–1013.
5. Huang, S.-Y.; Zhang, S.-H.; Liu, L.-L.; Zhu, W.-Q.; Cheng, Y.-M. Efficient slope reliability analysis and risk assessment based on multiple Kriging metamodels. *Comput. Geotech.* **2021**, *137*, 104277. [[CrossRef](#)]
6. Liu, L.L.; Cheng, Y.M. System reliability analysis of soil slopes using an advanced Kriging metamodel and quasi—Monte Carlo simulation. *Int. J. Geomech.* **2018**, *18*, 06018019. [[CrossRef](#)]
7. Cheng, Y.M.; Li, L.; Liu, L.L. Simplified approach for locating the critical probabilistic slip surface in limit equilibrium analysis. *Nat. Hazards Earth Syst. Sci.* **2015**, *15*, 1061–1112. [[CrossRef](#)]
8. Wang, Z.; Shafieezadeh, A. ESC: An efficient error-based stopping criterion for kriging-based reliability analysis methods. *Struct. Multidiscip. Optim.* **2019**, *59*, 1621–1637. [[CrossRef](#)]
9. Azhari, A.; Ozbaya, U. Investigating the effect of earthquakes on open pit mine slopes. *Int. J. Rock Mech. Min. Sci.* **2017**, *100*, 218–228. [[CrossRef](#)]
10. Feng, G.; Xia, Y.Y.; Wang, Z.D.; Yan, M. Dynamic early warning method of open-pit mine slopes based on integrated displacement information. *China Saf. Sci. J.* **2022**, *32*, 116–122.
11. Xu, Q.; Dong, X.J.; Li, W.L. Integrated Space-Air-Ground early detection, monitoring and warning system for potential catastrophic geohazards. *Geomat. Inf. Sci. Wuhan Univ.* **2019**, *44*, 957–966.
12. Karunathilake, A.; Zou, L.; Kikuta, K.; Nishimoto, M.; Sato, M. Implementation and configuration of GB-SAR for landslide monitoring: Case study in Minami-Aso, Kumamoto. *Explor. Geophys.* **2019**, *50*, 210–220. [[CrossRef](#)]
13. Du, Y.; Huang, G.W.; Zhang, Q. Asynchronous RTK method for detecting the stability of the reference station in GNSS deformation monitoring. *Sensors* **2020**, *20*, 1320. [[CrossRef](#)] [[PubMed](#)]
14. Basahel, H.; Mitri, H. Probabilistic assessment of rock slopes stability using the response surface approach—A case study. *Int. J. Min. Sci. Technol.* **2019**, *29*, 18–31. [[CrossRef](#)]
15. Li, D.Q.; Yang, Z.Y.; Cao, Z.J.; Zhang, L.M. Area failure probability method for slope system failure risk assessment. *Comput. Geotech.* **2019**, *107*, 36–44. [[CrossRef](#)]
16. Wang, L.; Wu, C.; Tang, L.; Zhang, W.; Lacasse, S.; Liu, H.; Gao, L. Efficient reliability analysis of earth dam slope stability using extreme gradient boosting method. *Acta Geotech.* **2020**, *15*, 313–3150. [[CrossRef](#)]
17. Zhang, W.; Wu, C.; Zhong, H.; Li, Y.; Lin, W. Prediction of undrained shear strength using extreme gradient boosting and random forest based on Bayesian optimization. *Geosci. Front.* **2021**, *12*, 469–477. [[CrossRef](#)]
18. Xu, X.H.; Shang, Y.Q.; Wang, Y.C. Global Stability Analysis of slope based on decision-making model of multi-attribute and interval number. *Chin. J. Rock Mech. Eng.* **2010**, *29*, 1840–1849. (In Chinese)
19. Cheng, M.Y.; Roy, A.F.V.; Chen, K.L. Evolutionary risk preference inference model using fuzzy support vector machine for road slope collapse prediction. *Expert Syst. Appl.* **2012**, *39*, 1737–1746. [[CrossRef](#)]
20. Hosseini, N.; Gholinejad, M. Investigating the Slope Stability Based on Uncertainty by Using Fuzzy Possibility Theory. *Arch. Min. Sci.* **2014**, *59*, 179–188. [[CrossRef](#)]
21. Park, H.J.; Um, J.G.; Woo, I.; Kim, J.W. Application of fuzzy set theory to evaluate the probability of failure in rock slopes. *Eng. Geol.* **2012**, *125*, 92–101. [[CrossRef](#)]
22. Liu, B.; Zhang, P.; Zhang, J.W. Analysis on slope stability of open-pit coal mine based on grey support vector machine. *Int. J. Smart Home* **2016**, *10*, 169–178. [[CrossRef](#)]
23. Wang, G.Y.; Cui, H.L.; Li, Q. Investigation of method for determining factors weights in evaluating slope stability based on rough set theory. *Rock Soil Mech.* **2009**, *30*, 2418–2422.
24. Li, Y.; Liu, J. Slope instability disaster forecast and its application based on RS-CPM model. *J. Cent. South Univ. (Sci. Technol.)* **2013**, *44*, 2971–2976.
25. Echard, B.; Gayton, N.; Lemaire, M. AK-MCS: An active learning reliability method combining Kriging and Monte Carlo Simulation. *Struct. Saf.* **2011**, *33*, 145–154. [[CrossRef](#)]
26. Liu, L.L.; Cheng, Y.M.; Wang, X.M. Genetic algorithm optimized Taylor Kriging surrogate model for system reliability analysis of soil slopes. *Landslides* **2017**, *14*, 535–546. [[CrossRef](#)]
27. Kim, J.; Song, J. Probability-Adaptive Kriging in n-Ball (PAK-Bn) for reliability analysis. *Struct. Saf.* **2020**, *85*, 101924. [[CrossRef](#)]
28. Zhan, W.; Lin, H.; Li, Z.L. Research on Security Risk Assessment System of Soil Slope Based on AHP. *Appl. Mech. Mater.* **2015**, *744*, 570–573. [[CrossRef](#)]
29. Zhang, J.; He, P.; Xiao, J.; Fei, X. Risk assessment model of expansive soil slope stability based on Fuzzy-AHP method and its engineering application. *Geomat. Nat. Hazards Risk* **2018**, *9*, 389–402. [[CrossRef](#)]
30. Zhao, C.; Cheng, G.P. Application of AHP in Material Selection in Slope Protection Project in Riverway. *Adv. Mater. Res.* **2013**, *683*, 921–924. [[CrossRef](#)]
31. Dos Santos, T.B.; Lana, M.S.; Pereira, T.M.; Canbulat, I. Quantitative hazard assessment system (Has-Q) for open pit mine slopes. *Int. J. Min. Sci. Technol.* **2019**, *29*, 419–427. [[CrossRef](#)]
32. Cheng, H.Z.; Chen, J.; Chen, R.P.; Chen, G.; Zhong, Y. Risk assessment of slope failure considering the variability in soil properties. *Comput. Geotech.* **2018**, *103*, 61–72. [[CrossRef](#)]
33. Pinheiro, M.; Sanches, S.; Miranda, T.; Neves, A.; Tinoco, J.; Ferreira, A.; Correia, A.G. A new empirical system for rock slope stability analysis in exploitation stage. *Int. J. Rock Mech. Min. Sci.* **2015**, *76*, 182–191. [[CrossRef](#)]

34. Yang, Z.P.; Zhou, X.L.; Hu, X. Decision on treatment schemes for highway slopes based on soft set theory. *Technol. Highw. Transp.* **2016**, *32*, 22–25. (In Chinese)
35. Zhou, X.; Sun, Y.; Huang, Z.; Yang, C.; Yen, G.G. Dynamic multi-objective optimization and fuzzy AHP for copper removal process of zinc hydrometallurgy. *Appl. Soft Comput.* **2022**, *129*, 109613. [[CrossRef](#)]
36. Qin, D.L.; Zhang, L.; Li, J.H. Risk Assessment Approach for Information Security Based on FAHP. *Comput. Eng.* **2009**, *35*, 156–158.
37. Chen, T.; Lin, Y.C.; Chiu, M.C. Approximating alpha-cut operations approach for effective and efficient fuzzy analytic hierarchy process analysis. *Appl. Soft Comput.* **2019**, *85*, 105855. [[CrossRef](#)]
38. Ahmed, F.; Kilic, K. Fuzzy Analytic Hierarchy Process: A performance analysis of various algorithms. *Fuzzy Sets Syst.* **2019**, *362*, 110–128. [[CrossRef](#)]
39. Zhang, Y.L.; Xu, H.W.; Liu, W.F. Interval-valued fuzzy parameterized soft sets and its applications in decision making. *J. Xihua Univ. Nat. Sci.* **2014**, *33*, 44–52.
40. He, X.; Du, Y.X.; Liu, W.F. Dynamic interval-valued fuzzy soft sets and their application to decision making. *J. Sichuan Univ. Sci. Eng. (Nat. Sci. Ed.)* **2015**, *28*, 92–96.
41. Zhu, J.; Xu, Y.; Chen, X.G. Interval-valued trapezoid fuzzy soft set and its properties. *J. Heilongjiang Univ. Sci. Technol.* **2016**, *26*, 332–335.
42. Acar, U.; Koyuncu, F.; Tanay, B. Soft sets and soft rings. *Comput. Math. Appl.* **2010**, *59*, 3458–3463. [[CrossRef](#)]
43. Maji, P.K.; Biswas, R.; Roy, A.R. Soft set theory. *Comput. Math. Appl.* **2003**, *45*, 555–562. [[CrossRef](#)]
44. Buckley, J.J.; Feuring, T.; Hayashi, Y. Fuzzy hierarchical analysis. *Fuzzy Sets Syst.* **1985**, *17*, 233–247. [[CrossRef](#)]
45. Chen, S.J.; Chen, S.M. Fuzzy risk analysis based on the ranking of generalized trapezoidal fuzzy numbers. *Appl. Intell.* **2007**, *26*, 1–11. [[CrossRef](#)]
46. Laarhoven, P.; Pedrycz, W. A fuzzy extension of Saaty's priority theory. *Fuzzy Sets Syst.* **1983**, *11*, 199–227. [[CrossRef](#)]